Body weight homeostat that regulates fat mass independently of leptin in rats and mice

John-Olov Jansson[a,1], Vilborg Palsdottir[a], Daniel A. Hägg[b], Erik Schéle[a], Suzanne L. Dickson[a], Fredrik Anesten[a], Tina Bake[a], Mikael Montelius[c], Jakob Bellman[a], Maria E. Johansson[a], Roger D. Cone[d,e], Daniel J. Drucker[f], Jianyao Wu[b], Biljana Aleksic[b], Anna E. Törnqvist[b], Klara Sjögren[b], Jan-Åke Gustafsson[g,1], Sara H. Windahl[b], and Claes Ohlsson[b,1]

[a]Department of Physiology, Institute of Neuroscience and Physiology, Sahlgrenska Academy, University of Gothenburg, SE 405 30, Gothenburg, Sweden; [b]Centre for Bone and Arthritis Research, Institute of Medicine, Sahlgrenska Academy, University of Gothenburg, SE 413 45, Gothenburg, Sweden; [c]Department of Radiation Physics, Institute of Clinical Sciences, Sahlgrenska Academy, University of Gothenburg, SE 413 45, Gothenburg, Sweden; [d]Life Sciences Institute, University of Michigan, Ann Arbor, MI 48109-2216; [e]Department of Molecular and Integrative Physiology, University of Michigan, Ann Arbor, MI 48109-2216; [f]Department of Medicine, Lunenfeld-Tanenbaum Research Institute, Mount Sinai Hospital, University of Toronto, ON M5G 1X5, Toronto, Canada; and [g]Department of Biology and Biochemistry, Center for Nuclear Receptors and Cell Signaling, University of Houston, Houston, TX 77204

Contributed by Jan-Åke Gustafsson, November 8, 2017 (sent for review September 7, 2017; reviewed by Wolfgang Langhans and Subburaman Mohan)

Subjects spending much time sitting have increased risk of obesity but the mechanism for the antiobesity effect of standing is unknown. We hypothesized that there is a homeostatic regulation of body weight. We demonstrate that increased loading of rodents, achieved using capsules with different weights implanted in the abdomen or s.c. on the back, reversibly decreases the biological body weight via reduced food intake. Importantly, loading relieves diet-induced obesity and improves glucose tolerance. The identified homeostat for body weight regulates body fat mass independently of fat-derived leptin, revealing two independent negative feedback systems for fat mass regulation. It is known that osteocytes can sense changes in bone strain. In this study, the body weight-reducing effect of increased loading was lost in mice depleted of osteocytes. We propose that increased body weight activates a sensor dependent on osteocytes of the weight-bearing bones. This induces an afferent signal, which reduces body weight. These findings demonstrate a leptin-independent body weight homeostat ("gravitostat") that regulates fat mass.

diet-induced obesity | weight loss | osteocytes | glucose metabolism

Epidemiologic studies demonstrate that subjects spending much time sitting have increased risk of obesity, diabetes, and cardiovascular diseases. There is even epidemiologic evidence for an association between sitting time and overall mortality (1, 2). The mechanism for the antiobesity effect of standing is essentially unknown. It is probable that part of the effect of high sitting time on cardiometabolic phenotypes is caused by the associated low degree of exercise. However, the results of some articles demonstrate that the association of a sedentary behavior, as reflected by much sitting time, with the metabolic syndrome, is independent of physical activity (3, 4). We hypothesized that there is a homeostat (5) in the lower extremities regulating body weight with an impact on fat mass. Such a homeostat would (together with leptin) ensure sufficient whole body energy depots but still protect land-living animals from becoming too heavy. A prerequisite for such homeostatic regulation of body weight is that the integration center, which may be in the brain, receives afferent information from a body weight sensor. Thereafter, the integration center may adjust the body weight by acting on an effector (6).

Results

Body Weight Sensing for Fat Mass Homeostasis in Mice with Diet-Induced Obesity. To investigate our hypothesis that there is a homeostatic regulation of body weight and fat mass based on loading, we implanted capsules that weighed 15% of the body weight into the abdomen of adult Sprague-Dawley rats and C57BL6 mice with diet-induced obesity (load). Control animals were implanted with an empty capsule of equal size (3% of the body weight). We found that increased loading suppressed the biological body weight both in rats and mice (Fig. 1 *A* and *B*). The difference in biological body weight between rodents with load and control rodents was first seen on day 2 after implantation and was larger on day 14 when the experiment was terminated (Fig. 1 *A* and *B*). At the end of the experiment the total body weight (= biological body weight + capsule weight) was rather similar in the load and control mice (Fig. S1*A*). Calculations of the efficiency of the homeostatic regulation of total body weight at 2 wk after initiation of the loading revealed that ~80% of the increased loading was counteracted by reduced biological weight (Fig. S1*B*). The increased loading also reduced the amount of white adipose tissue (WAT), as illustrated by representative MRI slices (Fig. 1*C*) and quantified by WAT dissection (Fig. 1*D*) and serum leptin levels (Fig. 1*E*). These findings demonstrate that there is an efficient body weight sensing mechanism for the homeostatic regulation of body weight.

The possible mechanism behind the suppression of body weight by increased loading was investigated on day 6 after implantation of capsules, a time point when the difference in body weight was still robustly increasing between load and control rodents (Fig. 1 *A* and *B*). There was no significant difference between mice with load and control mice in UCP1 mRNA levels in brown adipose tissue (BAT) (Fig. S1*C*), in oxygen consumption as a measure of energy expenditure (Fig. S1*D*), in respiratory quotient (RQ) (Fig. S1*E*), or in motor activity (Fig. S1*F*). Importantly, load decreased food intake, both calculated as percent of body weight (Fig. 1 *F*

Significance

The only known homeostatic regulator of fat mass is the leptin system. We hypothesized that there is a second homeostat regulating body weight with an impact on fat mass. In this study we have added and removed weight loads from experimental animals and measured the effects on the biological body weight. The results demonstrate that there is a body weight homeostat that regulates fat mass independently of leptin. As the body weight-reducing effect of increased loading was dependent on osteocytes, we propose that there is a sensor for body weight in the long bones of the lower extremities acting as "body scales." This is part of a body weight homeostat, "gravitostat," that keeps body weight and body fat mass constant.

Author contributions: J.-O.J., V.P., S.L.D., M.E.J., J.-Å.G., S.H.W., and C.O. designed research; V.P., D.A.H., E.S., F.A., T.B., M.M., J.B., J.W., B.A., A.E.T., K.S., and S.H.W. performed research; R.D.C. and D.J.D. contributed new reagents/analytic tools; J.-O.J., V.P., D.A.H., E.S., T.B., J.B., J.-Å.G., S.H.W., and C.O. analyzed data; and J.-O.J., V.P., J.-Å.G., S.H.W., and C.O. wrote the paper.

Reviewers: W.L., ETH Zurich; and S.M., Jerry L. Pettis Memorial VA Medical Center and Loma Linda University.

The authors declare no conflict of interest.

[1]To whom correspondence may be addressed. Email: joj@neuro.gu.se or jgustafs@central.uh.edu or Claes.Ohlsson@medic.gu.se.

This article contains supporting information online at www.pnas.org/lookup/suppl/doi:10.1073/pnas.1715687114/-/DCSupplemental.

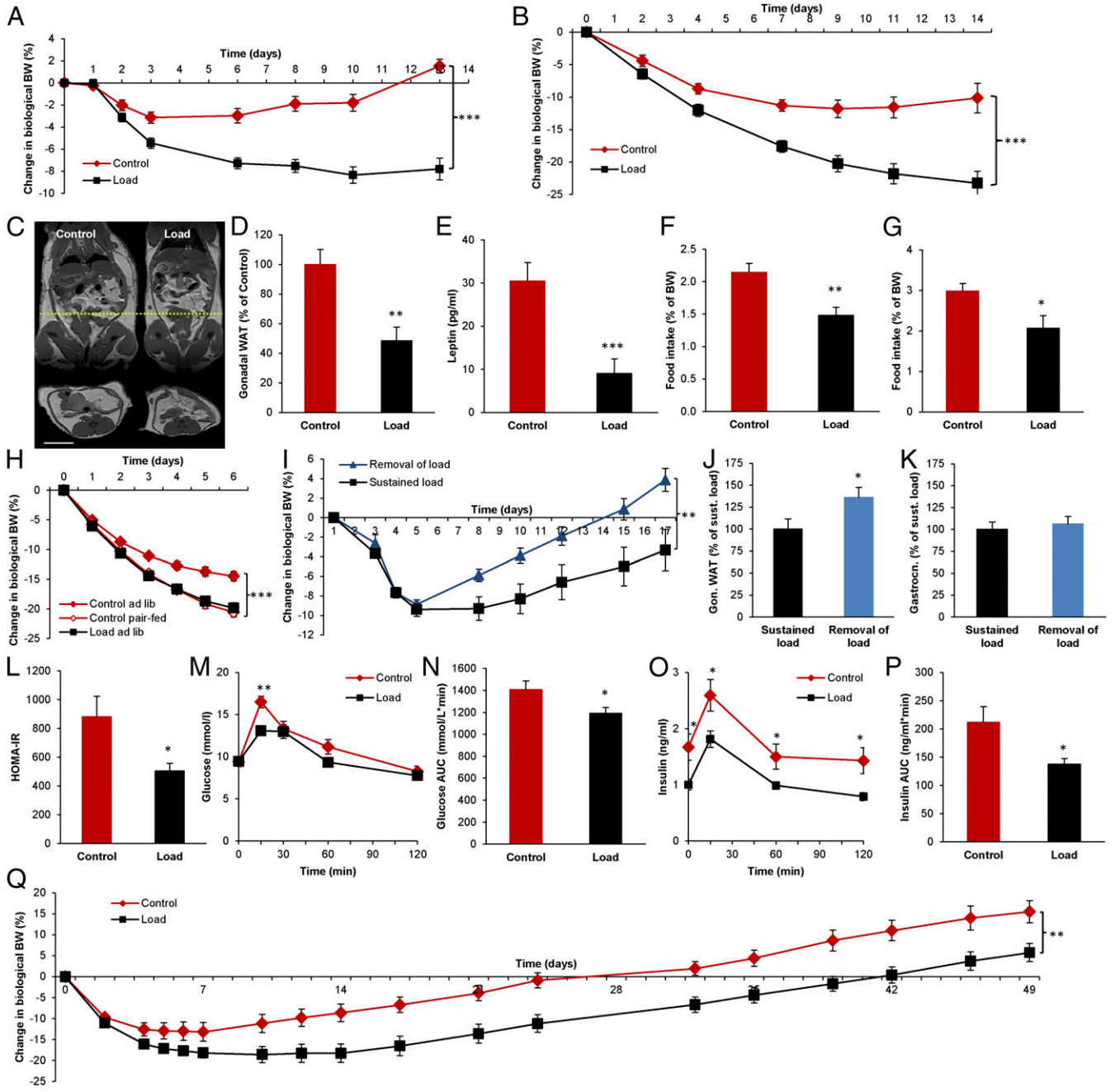

Fig. 1. Body weight sensing for fat mass homeostasis in rats and mice with diet-induced obesity. (*A*) Effect of loading on change in biological body weight (= total body weight − capsule weight) in rats ($n = 8$) and (*B*) mice ($n = 10$) implanted with capsules weighing 15% of the body weight (load) or empty capsules (control; ∼1.5% and ∼3% of the body weight for rats and mice, respectively). (*C*) Coronal (*Top*) and corresponding transversal (*Bottom*) MR images of a control (*Left*) and a load (*Right*) animal (day 14), acquired without fat suppression. Hyperintense regions represent body fat. Yellow dotted line and white bar indicate the position of the corresponding transversal images *Below* and 10 mm, respectively. (*D*) The fat mass (day 14), (*E*) the serum leptin levels (day 14), and (*F*) the food intake as percent of body weight (days 4–6) were measured in load and control rats ($n = 8$) and (*G*) mice ($n = 10$). (*H*) The effect of pair feeding on body weight change in control mice compared with ad libitum fed control and load mice ($n = 9$). (*I*) Change in biological body weight, (*J*) the fat mass (day 17), and (*K*) the skeletal muscle mass (day 17) after removal of load (heavy capsule followed by empty capsule) or sustained load (heavy capsule followed by heavy capsule) 14 d after the first implantation ($n = 10$). (*L*) HOMA-IR in fasted control and load mice ($n = 10$). (*M*) Blood glucose, (*N*) blood glucose area under the curve (AUC), (*O*) serum insulin, and (*P*) insulin AUC during an oral glucose tolerance test in load and control mice ($n = 10$). (*Q*) Effect of loading on long-term change in biological body weight in load and control mice ($n = 10$) followed during 7 wk after capsule implantation. Data are expressed as mean ± SEM $^*P < 0.05$, $^{**}P < 0.01$, $^{***}P < 0.001$.

and *G*) and calculated as food intake per animal in both rats and mice (Fig. S1 *G* and *H*).

Control mice pair fed with the same amount of food as the load mice decreased their body weight to the same extent as the load group (Fig. 1*H*). Therefore, the decreased biological body weight in the animals with increased loading did not seem to be caused primarily by increased energy expenditure, but rather by decreased food intake. An alternative loading procedure using capsules implanted s.c. on the back of the mice was also used. Increased loading suppressed the biological body weight in adult mice with diet-induced obesity also in this model (Fig. S1*I*). These experiments revealed that increased loading reduces the biological body weight.

We next evaluated whether reduced loading also influences the biological body weight by comparing mice with sustained loading (heavy capsule followed by heavy capsule) and mice with removal of loading (heavy capsule followed by empty capsule; Fig. 1*I*). Removal of the loading increased the biological body weight and the fat mass (Fig. 1*J*) but not the skeletal muscle mass (Fig. 1*K*), demonstrating that the body weight sensor is functional in both directions.

Loading improved insulin sensitivity as indicated by substantially reduced fasting homeostatic model assessment of insulin resistance (HOMA-IR) index (Fig. 1*L*) and reduced serum insulin before, during, and after oral glucose administration compared with control mice (Fig. 1 *O* and *P*). In addition, loading increased glucose tolerance as indicated by decreased levels of circulating glucose after oral glucose administration (Fig. 1 *M* and *N* and Fig. S1 *K* and *L*). Although loading reduced the absolute serum insulin levels throughout the glucose tolerance test (GTT) (Fig. 1 *O* and *P*), the induction of serum insulin from baseline was normal during the test (Fig. S1 *M* and *N*).

We also performed a long-term study, demonstrating that the effect of loading on biological body weight remained until the experiment was terminated at day 49 (Fig. 1*Q*).

Leptin-Independent Body Weight Sensing for Fat Mass Homeostasis. A prerequisite for homeostatic feedback regulation of energy depots in body fat tissue (energy balance) is that energy regulating parts of the brain receive information from fat tissue about its size. The fat-derived hormone leptin, discovered by Friedman and coworkers over 20 y ago, is so far the only known such afferent homeostatic factor (7–9). In the present study, we next investigated the interactions between increased loading, a stimuli normally reflecting increased body fat mass, and leptin. The loading-induced decrease in body weight was seen in leptin-deficient obese (Ob/Ob) mice (Fig. 2*A*), in the same way as in wild-type mice (Fig. 1*B*). In addition, the combined effect of increased loading and leptin treatment was studied in wild-type mice. Leptin was given to loaded and control mice on days 11–15 after implantation of capsules. It was found that leptin treatment suppressed body weight (Fig. 2*B*) and body fat (Fig. 2*C*) to a similar extent in loaded and control mice, while none of the treatments affected muscle mass (Fig. 2*D*). Thus, the loading-induced homeostatic regulation of body weight was independent of the well-established fat mass reducing effect of leptin, revealing two independent negative feedback systems for fat mass homeostasis.

Since the body weight reducing effect of increased loading was caused by reduced food intake, we analyzed the expression of appetite regulating genes in the hypothalamus. Increased loading augmented the expression of the obesity promoting neuropeptides AgRP and NPY (Fig. S1*J*). These two peptides are expressed by essentially the same neurons in the arcuate nucleus of the hypothalamus and their expression is suppressed by leptin. Therefore, the increase in AgRP and NPY expression is likely to be a failed compensatory mechanism induced by low fat mass and low serum leptin in the mice exposed to increased loading (Fig. 1 *D* and *E* and Fig. S1*J*), consistent with a leptin-independent mechanism for increased loading to reduce body weight.

The Suppression of Body Weight and Fat Mass by Loading Is Dependent on Osteocytes. It is known that osteocytes can sense dynamic short-term high-impact bone loading for local bone adaptation (10–12). We therefore postulated that chronic static moderately increased bone loading, induced by increased body weight, also activates osteocytes, and thereby reduces fat mass via a systemic signal. To determine the role of osteocytes for the suppression of body weight by increased loading, we established an osteocyte depleted transgenic mouse model using diphtheria toxin-driven cell depletion specifically of DMP1 positive osteocytes (Fig. S2). The normal suppression of body weight by increased loading observed in mice with intact osteocytes (Fig. 3*A*) was lost in osteocyte-depleted mice (Fig. 3*B*). Increased loading decreased the weight of WAT (Fig. 3*C*) and serum leptin levels (Fig. 3*D*) in mice with intact osteocytes but not in osteocyte-depleted mice, while there was no significant differences in the skeletal muscle weight between the groups (Fig. 3*E*). These findings demonstrate that the suppression of body weight by loading is dependent on osteocytes. We propose that increased body weight activates a sensor dependent on the osteocytes of the weight-bearing bones. This induces an afferent signal to reduce food intake (Fig. 3*F*).

A growing body of data indicates that the skeleton is an endocrine organ that regulates energy and glucose metabolism through, at least in part, the release of the bone-derived hormone osteocalcin (13, 14). We therefore hypothesized that the homeostatic regulation of body weight and fat mass by osteocytes in response to changes in

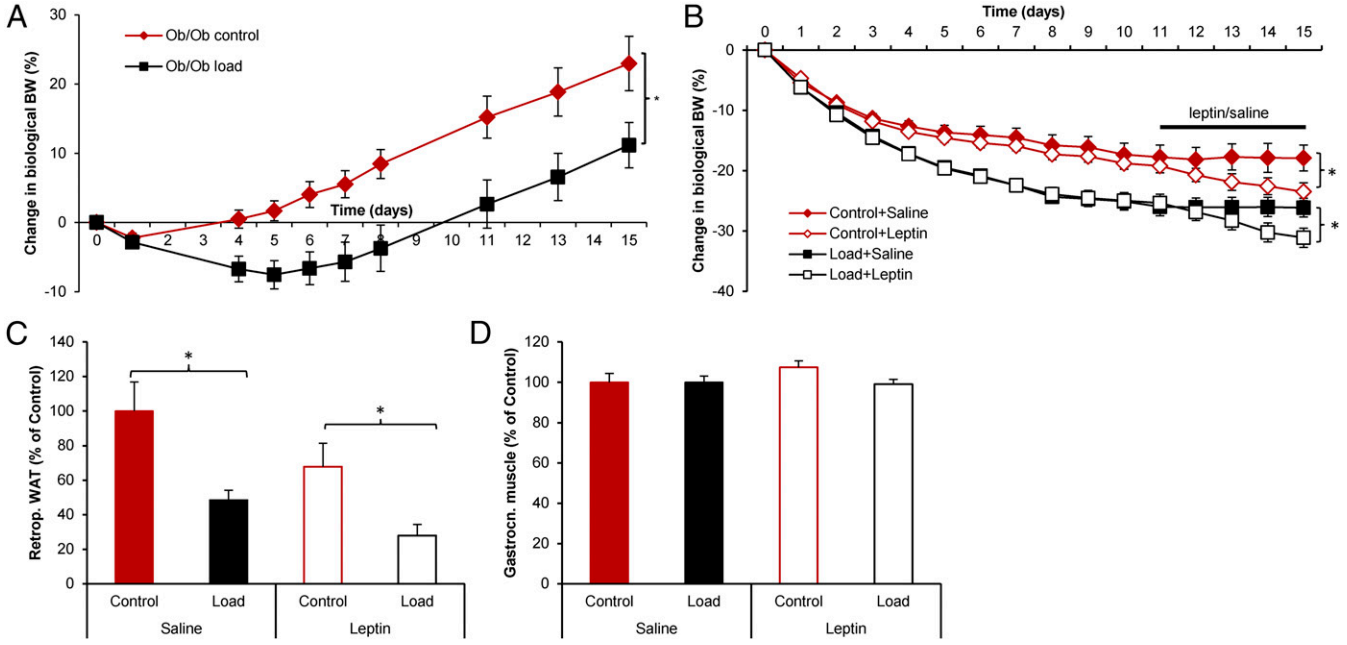

Fig. 2. Leptin-independent body weight sensing for fat mass homeostasis. (*A*) The effect of increased loading on the change in body weight in leptin deficient Ob/Ob mice (control $n = 7$ and load $n = 10$). The effect of combined loading and leptin treatment (1.5 μg/g BW twice daily) on (*B*) changes in biological body weight, (*C*) fat mass, and (*D*) muscle mass in mice ($n = 10$). Data are expressed as mean ± SEM *$P < 0.05$.

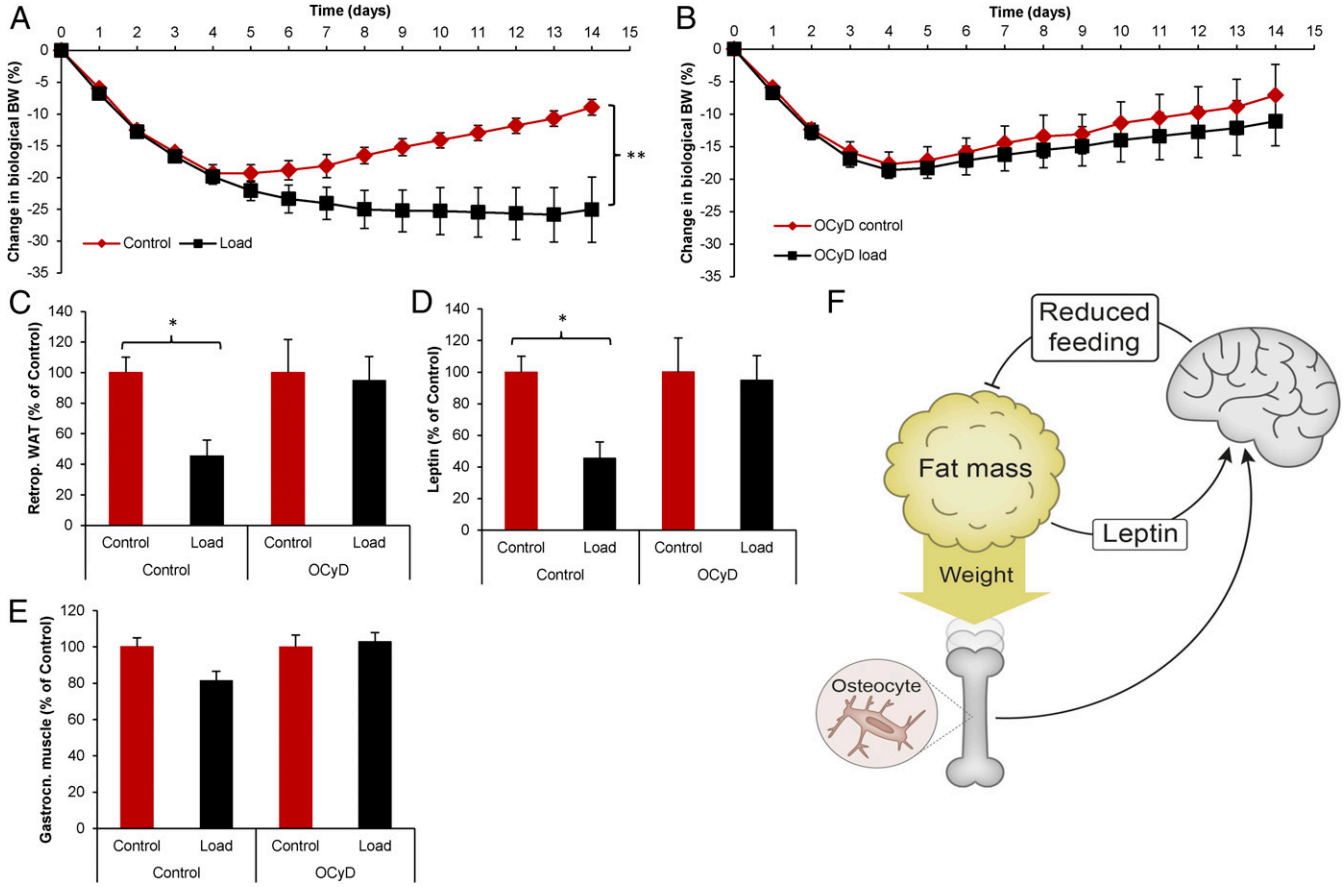

Fig. 3. The suppression of body weight and fat mass by loading is dependent on osteocytes. Effect of increased loading on change in biological body weight in (*A*) control female mice with intact osteocytes (control $n = 11$ and load $n = 12$) and in (*B*) osteocyte-depleted (OCyD) female mice ($n = 9$). The effect of loading of control mice with intact osteocytes and OCyD mice on (*C*) fat mass, (*D*) serum leptin levels, and (*E*) muscle mass, as measured 21 d after initiation of loading. Data are expressed as mean ± SEM $*P < 0.05$. (*F*) Hypothesis for homeostatic regulation of body fat mass by two different signal systems. The first previously known pathway is fat-derived leptin in circulation acting on the brain to decrease food intake and fat mass. The second mechanism is that increased fat mass is counteracted by the body weight homeostat (gravitostat). Increased body weight activates a sensor dependent on the osteocytes of the weight-bearing bones. This induces an afferent signal to reduce food intake.

body weight may be mediated by osteocalcin, or another known bone-derived circulating factor. To investigate this hypothesis, we determined the effect of increased loading for 6 d on the bone expression and circulating levels of four bone-derived candidate factors (sclerostin, osteocalcin, FGF23, and lipocalin 2) that might mediate this effect (Fig. S3). As previously shown for dynamic short-term high-impact loading, static moderately increased loading for 6 d reduced the bone expression of *Sost* (the gene coding for the bone mass suppressing factor sclerostin) (Fig. S3*A*). However, serum levels of sclerostin were not affected by increased loading (Fig. S3*B*). Although osteocalcin is a crucial regulator of energy metabolism in rodents, no effect of increased loading on the expression of osteocalcin in bone (Fig. S3*C*) or on circulating levels of total (Fig. S3*D*), carboxylated (Fig. S3*E*), or undercarboxylated (Fig. S3*F*) osteocalcin was observed. Furthermore, serum testosterone levels, known to be regulated by bone-derived osteocalcin and to regulate fat mass, were not affected by loading (15) (Fig. S3*G*). FGF23 is an osteocyte-derived endocrine acting factor. Increased loading did not significantly alter FGF23 expression in bone (Fig. S3*H*) or serum FGF23 levels (Fig. S3*I*). It was recently demonstrated that bone-derived lipocalin 2 suppresses appetite via a MC4R-dependent pathway (16). Increased loading did not significantly alter lipocalin 2 mRNA levels in bone (Fig. S3*J*) or serum lipocalin 2 levels in mice (Fig. S3*K*). These findings do not support that any of the four main bone-derived circulating candidate factors mediate the effect of the osteocyte-dependent body weight sensing mechanism.

Effect of Loading on Biological Body Weight in Relation to Other Known Body Fat Regulators. As described above (Fig. 2 *A*–*B*), the decrease in body weight by loading was independent of leptin. We next investigated the suppression of body weight by increased loading in relation to other known fat mass regulating signals (Fig. S4). To regulate fat mass, the hypothalamus needs afferent signals from the gastrointestinal tract, e.g., by the hunger and adiposity-inducing hormone ghrelin (17). We found that loading suppressed body weight in mice lacking the ghrelin receptor (Fig. S4*A*). Moreover, body weight was decreased by loading in mice lacking the receptor for glucagon-like peptide 1 (GLP-1) (Fig. S4*B*), an insulin-releasing hormone, described to regulate body weight (18). Thus, we found no evidence that loading is dependent on fat mass-regulating signals from the gastrointestinal tract. A major regulator of body fat in the hypothalamus is the circuit involving the neuropeptide α-MSH acting on the melanocortin receptor-4 (MC4R) (19, 20). The body weight decreasing effect of loading was also found in MC4R gene knockout mice (Fig. S4*C*). Therefore, the suppression of body weight by loading is independent of the α-MSH MC4R system, a major mediator of effects by leptin and GLP-1. Estrogen receptor-α (ER-α) signaling is involved in the regulation of both fat mass and bone mass. It has been shown that local bone formation induced by short-term high-impact loading is dependent on ER-α (10). However, our results from ER-α knockout mice indicate that ER-α is dispensable for the systemic regulation of body weight induced by chronical static moderately increased loading (Fig. S4*D*). We next determined whether neuronal signaling might mediate the loading-induced decrease in body weight. However, neither the sympathetic marker

noradrenaline in urine (Fig. S5*A*) nor the parasympathetic marker serum choline levels (Fig. S5*B*) were regulated by loading. These findings demonstrate that increased body weight activates a sensor dependent on the osteocytes of the weight-bearing bones. This induces an afferent food intake reducing signal that needs further study (Fig. 3*F*).

Discussion

The present findings reveal a body weight homeostat that regulates fat mass independently of leptin in rodents with diet-induced obesity. Increased body weight activates a sensor dependent on the osteocytes of the weight-bearing bones. This induces an afferent signal to reduce body weight.

We observed that increased loading decreased body weight, while decreased loading increases body weight, demonstrating that the body weight sensor is functional in both directions. Importantly, several authors have found that removal of fat by lipectomy causes a compensatory increase in fat mass and body weight in mice and rats lacking leptin activity (21–23). These data support our conclusion that a leptin-independent regulation of fat mass does exist, but they do not provide information about the possible mechanism. The present data, indicating that loading can regulate fat mass, raise the possibility that the increase in fat mass observed after lipectomy in leptin-deficient mice is due to decreased loading. Increased loading reduced the biological body weight via reduced food intake. The normal motor activity and the notion that the mice appeared healthy indicate that the effects of increased loading on food intake and body weight were specific.

It is well established that leptin signaling is necessary to prevent severe obesity (7, 24). However, most patients with obesity have high endogenous serum leptin levels and do not respond to exogenous leptin treatment. This indicates that, during these circumstances, leptin is not sufficient to suppress fat mass. This has been referred to as leptin resistance (7, 25).

We propose that both leptin signaling and body weight sensing are necessary for an optimal fat mass homeostasis. Pharmacologically, combined targeting of both the body weight sensing mechanism and leptin signaling may be useful for obesity treatment (Fig. 3*F*). In line with this, weight loading and leptin treatment suppressed body weight in an additive manner in the present study.

As described above, there is an established epidemiologic link between numbers of hours per day spent in the sitting position and several metabolic diseases, including obesity, diabetes, and cardiovascular diseases. However, the reason for this has been unknown (1, 2). We propose that much sitting time results in decreased loading of osteocytes in the weight-bearing long bones and, thereby, the homeostatic regulation of body weight does not activate its afferent signal to the brain, resulting in obesity (Fig. 3*F*). In addition, it is possible that secular trends of increased sitting time, via reduced activation of the body weight sensing mechanism, might have contributed to the obesity epidemic. The fact that loading was effective in decreasing fat mass in both Sprague-Dawley rats and C57BL mice with diet-induced obesity, well established models of clinical obesity (26, 27), suggests that increased standing time and, thereby, increased loading will be effective in decreasing human obesity. In addition, our findings demonstrate that loading increases insulin sensitivity. Further studies are needed to investigate whether this effect is completely or only partly due to decreased body fat mass.

The present findings reveal a body weight homeostat that regulates fat mass independently of leptin. We suggest that this body weight homeostat is called "gravitostat" (Latin gravis, meaning heavy; Latin status, meaning stable). The gravitostat, like other homeostats is based on communication between a sensor, an integration center, and an effector. Its sensor is most likely located in the weight-bearing lower extremities. Our data indicate that at least part of this sensor is in osteocytes. Increased fat mass is counteracted both by the gravitostat and by increased fat-derived leptin (7, 24) (Fig. 3*F*). The gravitostat activates an afferent signal for body weight homoeostasis to reduce food intake (Fig. 3*F*). Leptin has the capacity to decrease body weight, to some extent mediated by reduced food intake (7, 9). Therefore, both the gravitostat and leptin are eventually acting on the brain and seem to have their integrative centers there (Fig. 3*F*). Although both leptin and the gravitostat have the capacity to regulate fat mass, it has been proposed that the role of leptin primarily is in the lower end of fat mass homeostasis (25, 28), while the present data demonstrate that the gravitostat is efficient in diet-induced obesity. Future studies are warranted to determine whether activation of the gravitostat explains the beneficial effects of standing. Furthermore, when evaluated in a relevant disease model, it was observed that loading relieved diet-induced obesity and improved insulin sensitivity, suggesting the gravitostat is an interesting drug target for metabolic diseases (Fig. 3*F*).

Materials and Methods

Animals. All animal procedures were approved by the Ethics Committee on Animal Care and Use of Gothenburg University. C57BL/6 mice were purchased from Taconic, leptin-deficient Ob/Ob mice were purchased from The Jackson Laboratory and Ghrelin receptor knockout (GHSR KO) mice were obtained from Deltagen. MC4R KO mice, GLP-1R KO mice, and ERα KO mice were developed as previously described (19, 20, 29, 30). All knockout mice and their controls were on a C57BL/6 background. Sprague-Dawley rats were purchased from Charles River Laboratories.

To generate the osteocyte-depleted mice, DMP-1 promoter-Cre mice (31) were crossed with ROSA26 promoter-Flox-STOP-Flox-DTR mice (32) (Fig. S2). Diphtheria toxin receptor (DTR) mRNA was compared between cortical bone, kidney, and liver with RT-PCR (Fig. S2*C*). Sost mRNA was measured in cortical bone as a marker of osteocyte depletion (OCyD) in mice expressing DTR and given diphtheria toxin (Fig. S2*D*).

Immunohistochemistry. The number of osteocytes and empty osteocyte lacunae in femur was evaluated blinded using a bright field microscope. Briefly, femur was fixed, paraffin embedded, sectioned, and stained with hematoxylin and eosin. Three evenly spread out sections of femur were used for counting. Osteocytes and empty lacunae were counted from cortical bone covering on average 0.16 mm^2 per section and located 5 mm from the tip of the epiphyseal plate. The number of apoptotic osteocytes was measured as cells with TUNEL positive staining. Briefly, three femur sections neighboring the sections used for counting empty lacunae were stained using TUNEL assay (ApopTag Fluorescein In Situ Apoptosis Detection Kit, S7110; Millipore) in accordance with instructions provided and counterstained with DAPI. Using a wide field fluorescent microscope (Leica DMRB; Leica Microsystems), images were taken covering on average 0.16 mm^2 of cortical bone per section and located 5 mm from the tip of the epiphyseal plate. Background autofluorescence was reduced by applying a digital channel subtraction method to the images. TUNEL positive cells and DAPI positive cells were counted within the images.

In a separate experiment, blue β-gal staining of femoral bone sections was used as a marker of cells with active DMP-1 promoter. DMP-1 promoter-Cre mice or wild-type mice were crossed with ROSA26 promoter-Flox-STOP-Flox-β-gal mice. The staining with β-gal in cortical bone was compared between ROSA26 promoter-Flox-STOP-Flox-β-gal mice with and without DMP-1 promoter-Cre.

Loading. Two- to 3-mo-old mice and rats were fed a high-fat diet (60% fat, D12492; Research Diets) during 4 wk and then a capsule that weighed 15% of the body weight (load) or 3% of the body weight (control) was implanted intraperitoneally or s.c. into the adult animals under isoflurane anesthesia. After the implantation, the body weight was measured daily or several times per week until the end of each experiment.

Removal of load was done in one experiment in which the capsules were exchanged 2 wk after the first surgery and half of the mice with load capsules got control capsules (removal of load) and half of them got new load capsules (sustained load) with a follow-up period of 3 wk after removal of load.

Indirect Calorimetry, Food Intake, and Activity Measurement. Oxygen consumption and carbon dioxide production was measured by indirect calorimetry in an INCA Metabolic System (Somedic) as previously described (33). The RQ was calculated by the formula RQ = VCO2/VO2. The measurement was done on days 4–6 after implantation of capsules in C57BL/6 mice and the food intake was monitored during the same period for both mice and rats. We also performed a pair feeding study, in which we fed control mice the same amount of food as ad libitum fed load mice. The motor activity was measured in automated activity chambers, so-called Locoboxes, consisting of a plastic cage (55 × 55 × 22 cm) inside a ventilated cabinet (Kungsbacka Mat-och Reglerteknik AB).

Glucose Tolerance Test. Oral GTT was performed on C57BL/6 mice 3 wk after capsule implantation. The mice received oral glucose [2 g/kg body weight (BW); Fresenius Kabi] by gavage after 5 h of fasting. Blood samples were collected from

the tail vein at 0, 15, 30, 60, and 120 min after the glucose gavage. Blood glucose concentrations were determined at the above-mentioned time points using an Accu-Check Compact Plus glucometer (Roche Diagnostics). Serum insulin concentrations were measured at time points 0, 15, 60, and 120 min after the glucose administration using the Ultrasensitive Mouse Insulin ELISA kit (90080; Chrystal Chem, Inc.) according to the protocol provided by the manufacturer.

Leptin Treatment. Control and loaded C57BL/6 mice were given murine leptin (1.5 μg/g BW; Pepro-Tech) or saline twice daily in s.c. injections on days 11–15 after the capsule implantation.

Gene Expression. Cortical bone from femur and tibia, hypothalamus, and interscapular BAT were dissected, snap frozen in liquid nitrogen, and kept in −80 °C until analysis. The cortical bones were homogenized with TriZol reagent (Invitrogen) before extraction. mRNA from all tissues was extracted using RNeasy Lipid Tissue Mini Kit (Qiagen) and the mRNA concentration of the samples was measured by NanoDrop spectrophotometry. cDNA was synthesized from 1 μg mRNA with iScript cDNA Synthesis Kit (Bio-Rad).

Real-time PCR was performed using Step-One-Plus or the ABI Prism 7900 Sequence Detection System (Applied Biosystems). The hypothalamus samples were analyzed with Universal Taqman Master Mix (Applied Biosystems) in a 48-gene custom-made TaqMan low-density array card and normalized to glyceraldehyde-3-phosphate dehydrogenase (GAPDH, Mm99999915_g1). The cortical bone samples were analyzed by assays for osteocalcin (Mm01741771_g1), sclerostin (Mm00470479_m1), FGF23 (Mm00445621_m1), and lipocalin 2 (Mm 01324470_m1) and normalized to 18S (4310893E). The BAT samples were analyzed with an assay for Ucp1 (Mm0124486_m1) and normalized to 18S (4310893E). The relative mRNA levels were obtained by using the comparative threshold cycle (Ct) method and calculated with the ΔΔCt equation.

Serum and Urine Analyses. Blood samples were collected at the end of each experiment and the serum was separated and kept in −80 °C until analysis. Serum was analyzed in duplicates by ELISAs for leptin (Chrystal Chem, Inc), sclerostin (ALPCO immunoassays), osteocalcin (Immutopics), Gla-osteocalcin and Glu-osteocalcin (Takara Clontech), FGF23 (Kainos Laboratories, Inc), lipocalin 2 (R&D Systems), and choline (Abcam). Serum testosterone was analyzed by a gas chromatography-tandem mass spectrometry method as previously described (34). Urine samples were analyzed by ELISA for noradrenaline (Labor Diagnostika Nord) and the urine was also analyzed for creatinine (Crystal Chem, Inc) to normalize the noradrenaline levels.

MRI. A 7T MR system (software: ParaVision 5.1; Bruker BioSpin MRI GmbH) and a 50-mm quadrature transmit/receive volume coil (RAPID Biomedical GmbH) were used to produce coronal images of each animal separately and transversal images of pairs of animals from the load and control groups. The pairing ensured identical MRI signal enhancement characteristics for both groups, to facilitate subsequent comparison of body fat content.

The coronal images were acquired using a 2D multi slice multi echo (MSME) sequence with repetition time (TR) = 1,000 ms, echo time (TE) = 12.3 ms, number of signal averages (NSA) = 2, slice thickness = 1 mm, field of view (FOV) (read × phase) = 64 × 28 mm^2, in-plane resolution = 160 × 160 mm^2, and receiver bandwidth (BW) = 120 kHz. The transversal images were acquired with slightly adjusted acquisition parameters (MSME sequence: TR = 1,000 ms, TE = 9.5 ms, NSA = 45, slice thickness = 0.7 mm, FOV = 46 × 35 mm^2, in-plane resolution = 177 × 177 mm^2 and BW = 120 kHz). Both coronal and transversal image series were acquired twice, with and without fat suppression, and coronal images were resampled to 177 × 177 mm^2 for visualization purposes. Regions of hyperintense MR signal (relative to muscle and organs) in a nonfat suppressed image were assumed to represent fat if the corresponding region in the fat-suppressed image was hypointense.

Statistics. Data were analyzed using two-tailed Student's *t* test assuming equal variance between control and load groups or between "sustained load" and "removal of load" groups. When more than two groups were compared, ANOVA followed by Tukey's post hoc test was used. $P < 0.05$ was considered statistically significant. All data are presented as mean ± SEM.

Data Availability Statement. The authors declare that all data supporting the findings of this study are available within the paper and its *Supporting Information* files.

ACKNOWLEDGMENTS. We thank Dr. Mikael Johansson (Department of Languages and Literatures, Gothenburg University) for advice regarding linguistics and senior research engineer Staffan Berg (Department of Neuroscience and Physiology, Gothenburg University) for development of loading capsules. This work was supported by the NovoNordisk Foundation, the Swedish Research Council, the Swedish Government [under the Avtal om Läkarutbildning och Medicinsk Forskning (Agreement for Medical Education and Research)], the Knut and Alice Wallenberg Foundation, EC Framework 7, and the Torsten Söderbergs Foundation.

1. Katzmarzyk PT, Church TS, Craig CL, Bouchard C (2009) Sitting time and mortality from all causes, cardiovascular disease, and cancer. *Med Sci Sports Exerc* 41:998–1005.
2. Levine JA, et al. (2005) Interindividual variation in posture allocation: Possible role in human obesity. *Science* 307:584–586.
3. Chau JY, van der Ploeg HP, Merom D, Chey T, Bauman AE (2012) Cross-sectional associations between occupational and leisure-time sitting, physical activity and obesity in working adults. *Prev Med* 54:195–200.
4. Ekblom Ö, et al. (2015) Cardiorespiratory fitness, sedentary behaviour and physical activity are independently associated with the metabolic syndrome, results from the SCAPIS pilot study. *PLoS One* 10:e0131586.
5. Bernard C (1865) *Introduction à l'Etude de la Médecine Expérimentale* (Flammarion, Paris).
6. Vander AJ (1990) Homeostatic mechanisms and cellular communication. *Human Physiology: The Mechanisms of Body Function*, eds Nunes I, Schanck DT, Bradley JW (McGraw-Hill, New York), 5th Ed, pp 141–166.
7. Friedman JM, Halaas JL (1998) Leptin and the regulation of body weight in mammals. *Nature* 395:763–770.
8. Zeng W, Lu YH, Lee J, Friedman JM (2015) Reanalysis of parabiosis of obesity mutants in the age of leptin. *Proc Natl Acad Sci USA* 112:E3874–E3882.
9. Zhang Y, et al. (1994) Positional cloning of the mouse obese gene and its human homologue. *Nature* 372:425–432.
10. Lee K, Jessop H, Suswillo R, Zaman G, Lanyon L (2003) Endocrinology: Bone adaptation requires oestrogen receptor-alpha. *Nature* 424:389.
11. Meakin LB, Price JS, Lanyon LE (2014) The contribution of experimental in vivo models to understanding the mechanisms of adaptation to mechanical loading in bone. *Front Endocrinol (Lausanne)* 5:154.
12. Vanderschueren D, et al. (2014) Sex steroid actions in male bone. *Endocr Rev* 35:906–960.
13. Ferron M, et al. (2010) Insulin signaling in osteoblasts integrates bone remodeling and energy metabolism. *Cell* 142:296–308.
14. Lee NK, et al. (2007) Endocrine regulation of energy metabolism by the skeleton. *Cell* 130:456–469.
15. Oury F, et al. (2011) Endocrine regulation of male fertility by the skeleton. *Cell* 144:796–809.
16. Mosialou I, et al. (2017) MC4R-dependent suppression of appetite by bone-derived lipocalin 2. *Nature* 543:385–390.
17. Tschöp M, Smiley DL, Heiman ML (2000) Ghrelin induces adiposity in rodents. *Nature* 407:908–913.
18. Holst JJ (2007) The physiology of glucagon-like peptide 1. *Physiol Rev* 87:1409–1439.
19. Butler AA, et al. (2001) Melanocortin-4 receptor is required for acute homeostatic responses to increased dietary fat. *Nat Neurosci* 4:605–611.
20. Huszar D, et al. (1997) Targeted disruption of the melanocortin-4 receptor results in obesity in mice. *Cell* 88:131–141.
21. Chlouverakis C, Hojnicki D (1974) Lipectomy in obese hyperglycemic mice (ob-ob). *Metabolism* 23:133–137.
22. Harris RB, Hausman DB, Bartness TJ (2002) Compensation for partial lipectomy in mice with genetic alterations of leptin and its receptor subtypes. *Am J Physiol Regul Integr Comp Physiol* 283:R1094–R1103.
23. Liszka TG, Dellon AL, Im M, Angel MF, Plotnick L (1998) Effect of lipectomy on growth and development of hyperinsulinemia and hyperlipidemia in the Zucker rat. *Plast Reconstr Surg* 102:1122–1127.
24. Montague CT, et al. (1997) Congenital leptin deficiency is associated with severe early-onset obesity in humans. *Nature* 387:903–908.
25. Frederich RC, et al. (1995) Leptin levels reflect body lipid content in mice: Evidence for diet-induced resistance to leptin action. *Nat Med* 1:1311–1314.
26. Kanasaki K, Koya D (2011) Biology of obesity: Lessons from animal models of obesity. *J Biomed Biotechnol* 2011:197636.
27. Wang CY, Liao JK (2012) A mouse model of diet-induced obesity and insulin resistance. *Methods Mol Biol* 821:421–433.
28. Myers MG, Cowley MA, Münzberg H (2008) Mechanisms of leptin action and leptin resistance. *Annu Rev Physiol* 70:537–556.
29. Dupont S, et al. (2000) Effect of single and compound knockouts of estrogen receptors alpha (ERalpha) and beta (ERbeta) on mouse reproductive phenotypes. *Development* 127:4277–4291.
30. Scrocchi LA, et al. (1996) Glucose intolerance but normal satiety in mice with a null mutation in the glucagon-like peptide 1 receptor gene. *Nat Med* 2: 1254–1258.
31. Lu Y, et al. (2007) DMP1-targeted Cre expression in odontoblasts and osteocytes. *J Dent Res* 86:320–325.
32. Soriano P (1999) Generalized lacZ expression with the ROSA26 Cre reporter strain. *Nat Genet* 21:70–71.
33. Wernstedt I, et al. (2006) Reduced stress- and cold-induced increase in energy expenditure in interleukin-6-deficient mice. *Am J Physiol Regul Integr Comp Physiol* 291: R551–R557.
34. Nilsson ME, et al. (2015) Measurement of a comprehensive sex steroid profile in rodent serum by high-sensitive gas chromatography-tandem mass spectrometry. *Endocrinology* 156:2492–2502.

Supporting Information

Jansson et al. 10.1073/pnas.1715687114

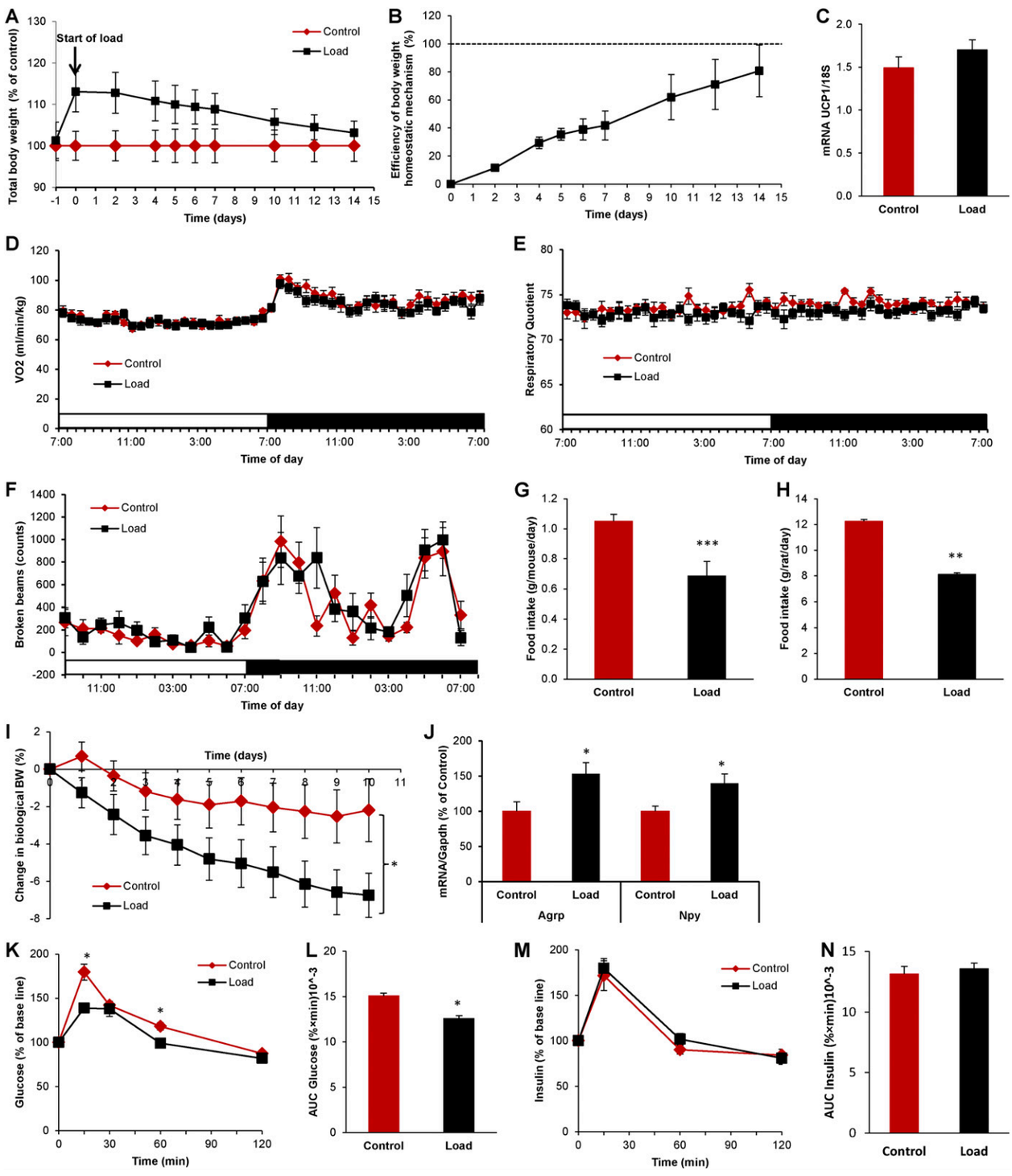

Fig. S1. Increased loading suppresses total body weight and food intake. (*A*) The effect of increased loading on the change in total body weight, including both the biological weight and the capsule weight. (*B*) The efficiency of the homeostatic regulation of total body weight calculated as: [(percent reduction in biological body weight in load mice – average percent reduction in biological body weight in control mice)/12] × 100, (n = 10). On days 4–6 after implantation of the capsules, (*C*) UCP1 mRNA in brown adipose tissue, (*D*) oxygen consumption in relation to biological body weight, (*E*) respiratory quotient, (*F*) motor activity, and (*G*) food intake were measured in control and load mice (n = 10) and (*H*) food intake was measured in rats (n = 8). (*I*) The change in body weight after an alternative loading procedure using control or load capsules implanted s.c. on the back of the mice (n = 10). (*J*) The effect of increased loading on hypothalamic mRNA expression of Agrp and Npy normalized to GAPDH (n = 10). (*K*) Glucose levels, (*L*) glucose area under the curve (AUC), (*M*) insulin levels, and (*N*) insulin AUC during oral glucose tolerance test, expressed as percent change from base line (n = 10). Data are expressed as mean ± SEM *P < 0.05, **P < 0.01, ***P < 0.001.

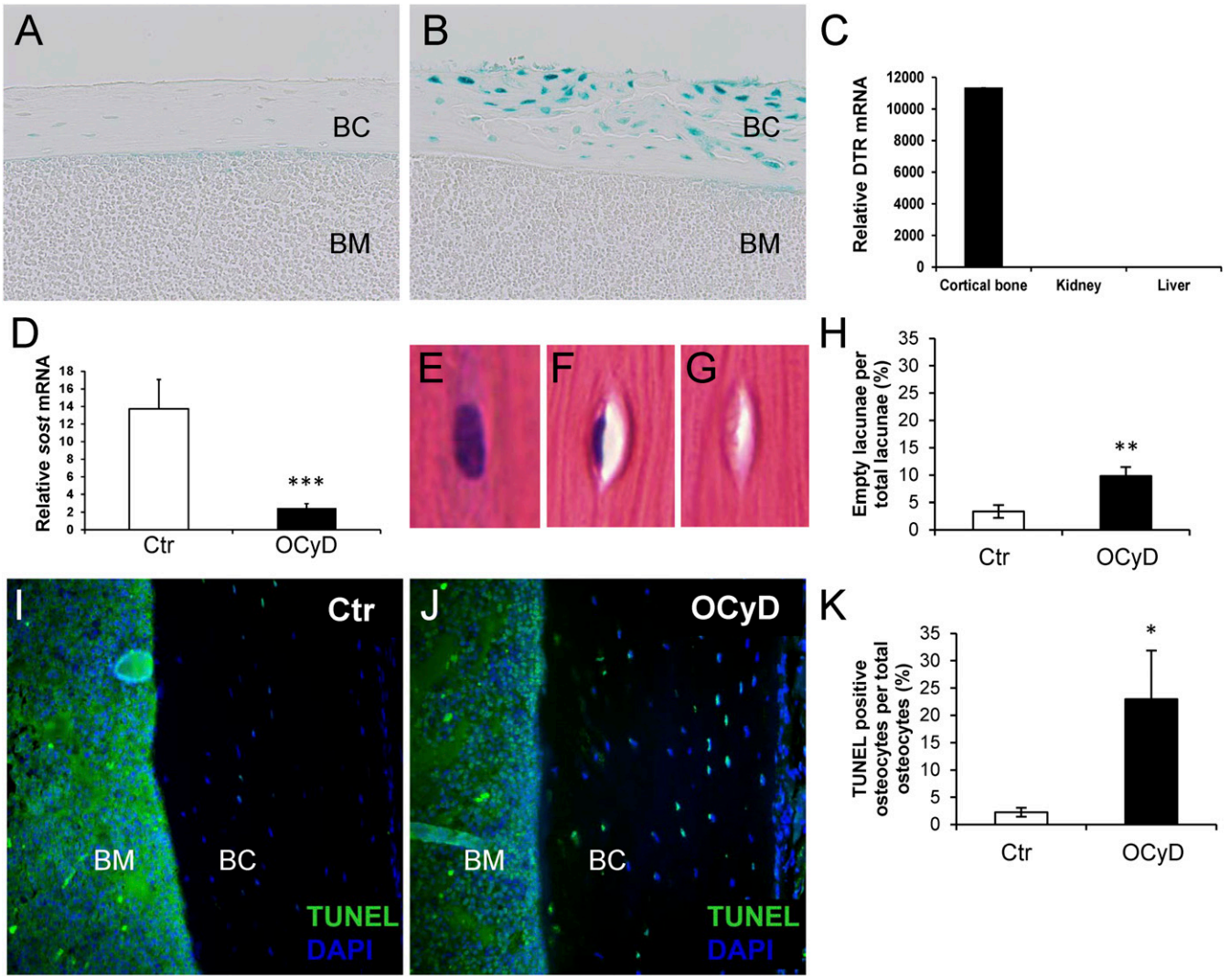

Fig. S2. Depletion of osteocytes. (*A* and *B*) Osteocyte specificity of the DMP-1 promoter-Cre mice used to achieve depletion of osteocytes. DMP-1 promoter-Cre mice were crossed with ROSA26 promoter-Flox-STOP-Flox-β-gal mice. Blue β-gal staining of femoral bone sections was used as a marker of cells with active DMP-1 promoter. There was little/no staining with β-gal in ROSA26 promoter-Flox-STOP-Flox-β-gal control mice without DMP-1 promoter-Cre (*A*), while marked specific staining was observed in osteocytes of the cortical bone of mice with DMP-1 promoter-Cre (*B*). (*C*–*K*) DMP-1 promoter-Cre mice were crossed with ROSA26 promoter-Flox-STOP-Flox-DTR mice to generate osteocyte-depleted (OCyD) mice upon diphtheria toxin administration. (*C*) Diphtheria toxin receptor (DTR) mRNA levels (HBGEF) were high specifically in cortical bone ($n = 5$). (*D*) Sost mRNA levels ($n = 6$) were decreased in cortical bone of OCyD mice expressing DTR and given diphtheria toxin compared with control mice without DTR (Ctr) given diphtheria toxin. (*E*–*G*) Examples of (*E*) filled lacuna, (*F*) partially empty lacuna, and (*G*) empty lacuna. (*H*) The number of completely empty osteocyte lacunae is increased in the OCyD mouse cortical bone ($n = 6$) compared with Ctr ($n = 5$). (*I*–*K*) Increased number of apoptotic osteocytes in the OCyD mouse cortical bone compared with Ctr. (*I* and *J*) Representative images showing fewer apoptotic cells in cortical bone of Ctr mice (*I*) compared with OCyD mice (*J*). TUNEL stain (green) indicates apoptotic cells. DAPI stain (blue) indicates nuclei of all cells. (*K*) The number of apoptotic osteocytes is increased in cortical bone from the OCyD mice ($n = 6$) compared with Ctr ($n = 5$). BC, bone cortex; BM, bone marrow. $^{*}P < 0.05$, $^{**}P < 0.01$, $^{***}P < 0.001$, OCyD vs. Ctr.

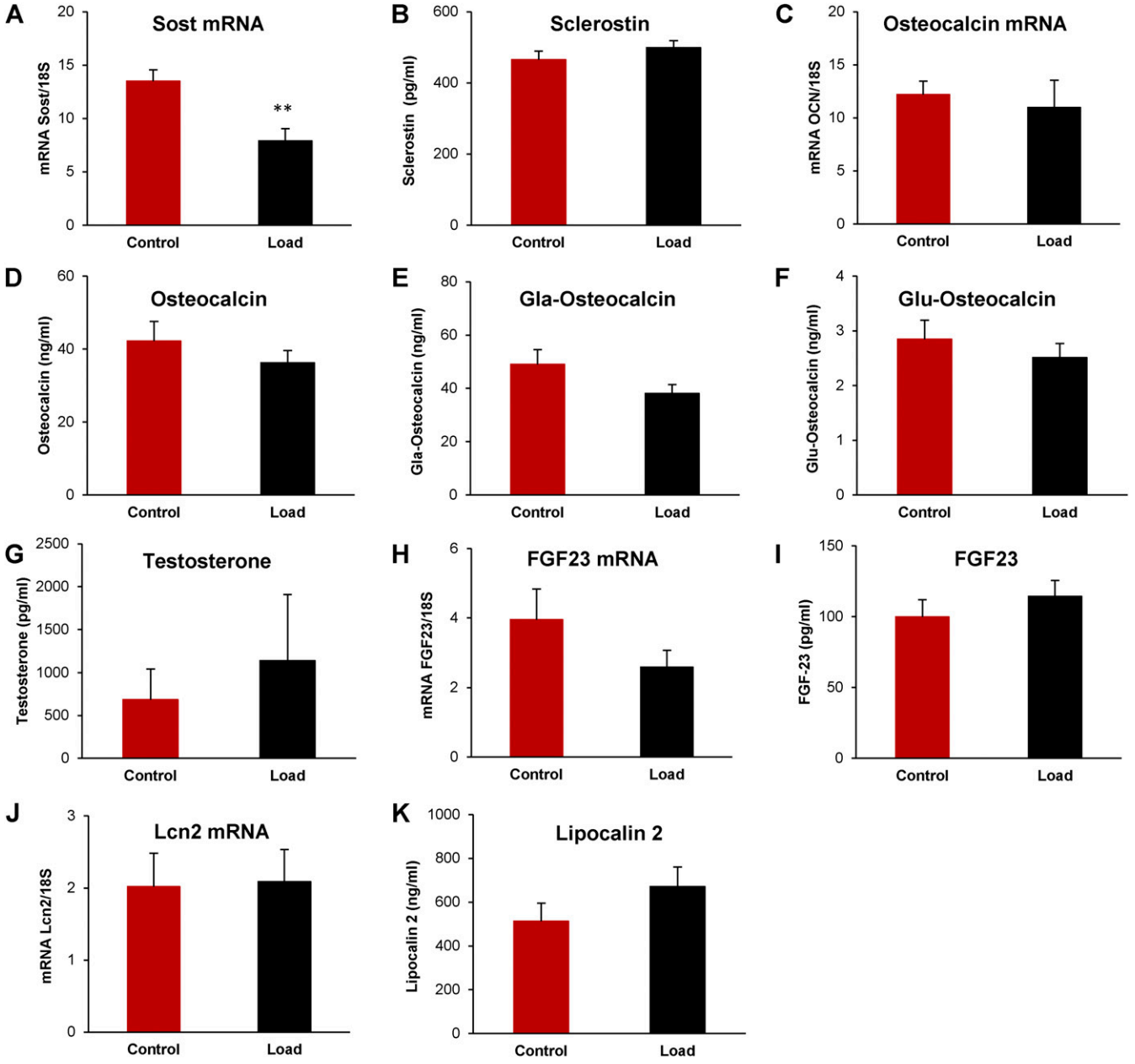

Fig. S3. Effect of loading on bone-derived endocrine factors and testosterone. The effect of loading on (*A*) the mRNA expression in cortical bone of Sost (the sclerostin gene), (*B*) serum levels of sclerostin, (*C*) mRNA levels in cortical bone of osteocalcin, (*D*) serum levels of total osteocalcin, (*E*) carboxylated osteocalcin (Gla-osteocalcin), (*F*) undercarboxylated osteocalcin (Glu-osteocalcin), (*G*) serum levels of testosterone, (*H*) mRNA levels of FGF23, (*I*) serum levels of FGF23, (*J*) mRNA levels of lipocalin 2 (Lcn2), and (*K*) serum levels of lipocalin 2, 6 d after initiation of loading ($n = 10$). Data are expressed as mean ± SEM $^{**}P < 0.01$.

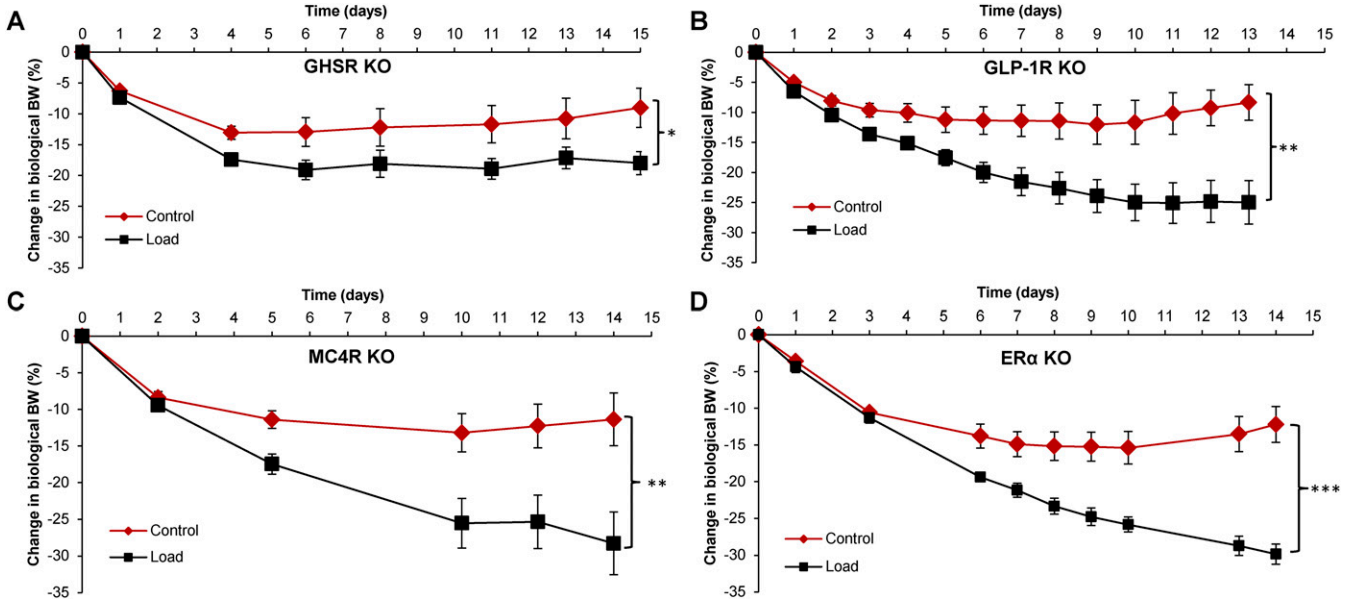

Fig. S4. Effect of loading on biological body weight in relation to other body fat regulators. Effect of loading on the change in biological body weight in (*A*) ghrelin receptor (GHSR) knockout mice (control $n = 4$ and load $n = 5$), (*B*) glucagon-like peptide-1 receptor (GLP-1R) knockout mice ($n = 8$), (*C*) melanocortin-4 receptor (MC4R) knockout mice ($n = 6$), and (*D*) estrogen receptor-α (ER-α) knockout mice ($n = 8$). Data are expressed as mean ± SEM $^*P < 0.05$, $^{**}P < 0.01$, $^{***}P < 0{,}001$.

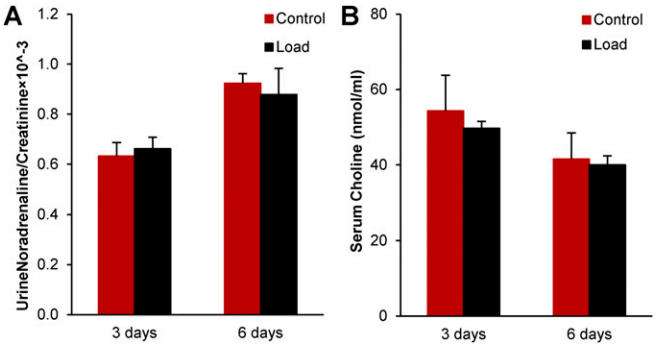

Fig. S5. Effect of loading on nervous transmitters. The effect of loading on (*A*) noradrenaline in the urine and (*B*) total choline in the serum from control and load mice 3 and 6 d after implantation of capsules (3 d, $n = 10$; 6 d control $n = 10$ and load $n = 9$). Data are expressed as mean ± SEM.